Structural Engineering and Mechanics, Vol. 8, No. 5 (1999) 439-452
DOI: http://dx.doi.org/10.12989/sem.1999.8.5.439

A boundary element approach for quasibrittle fracture propagation analysis

F. Tin-Loi†

School of Civil and Environmental Engineering, University of New South Wales, Sydney 2052, Australia

Abstract. A simple numerical scheme suitable for tracing the fracture propagation path for structures idealized by means of Hillerborg's classical cohesive crack model is presented. A direct collocation, multidomain boundary element method is adopted for the required space discretization. The algorithm proposed is necessarily iterative in nature since the crack itinerary is *a priori* unknown. The fracture process is assumed to be governed by a path-dependent generally nonlinear softening law. The potentialities of the method are illustrated through two examples.

Key words: cohesive crack; crack propagation; quasibrittle fracture; softening.

1. Introduction

This paper addresses the important and difficult problem of tracing the statical fracture propagation path for quasibrittle structures. In particular, we outline a simple numerical scheme suitable for carrying out this analysis for plane stress quasibrittle fracture processes where mode I is dominant. Under the usual assumptions of small deformations and linear elasticity outside the process zone (or craze), we describe the path-dependent softening law, characterizing the fracture processes, by means of a fairly general nonlinear softening function which admits, as special cases, the well-known single or bilinear branch representations. The path-dependent assumption is analogous to the flow theory of plasticity and hence enables elastic unloading from a softened state to be identified.

As can be construed from our introductory remarks, the model we use is the discrete crack idealization proposed by various researchers, *in primis* by Dugdale (1960), Barenblatt (1962) and, Hillerborg *et al.* (1976); the latter work specifically deals with concrete-like materials. In order to take advantage of the fact that such a model relegates all nonlinearity to a discontinuity locus, the space discretization is carried out within a multizone boundary element (BE) framework, with the interface zone representing the crack propagation itinerary. Following previous related work (Harder 1990, Liang and Li 1991a, 1991b, Cen and Maier 1992, Tin-Loi and Ferris 1997), we use the direct collocation method in view of its simplicity, although we must admit that the symmetric Galerkin BE approach may be more accurate and is physically more meaningful (Maier and Frangi 1998).

The organization of this paper is as follows. In Section 2, we review the cohesive crack model with the specific aim of describing a general class of nonlinear path-dependent fracture laws in a form suitable for our solution algorithm. The multizone BE formulation is presented next in Section 3. A key idea of the general scheme is to express the tractions at the crack interface as the sum of the tractions due to displacement discontinuities only and of tractions caused by the purely elastic response of an assumed uncracked structure under the given loads. The total tractions must then of course obey the appropriate constitutive law. We propose in Section 4 a simple numerical algorithm capable of solving the fracture problem in point. In particular, we describe schemes required for the necessary marching solution (for an assumed crack itinerary) and for adjusting the crack interface. The marching solution uses a classical Newton's method to solve a set of equations selected on the basis of an assumed crack pattern for the particular load level considered. The interface adjustment is based on a principal stress criterion. We illustrate application of the method in Section 5 by means of two examples before concluding with some remarks.

2. Cohesive crack law

As is well-known, the cohesive crack model (Hillerborg 1976) is a popular idealization of fracture processes regarding quasibrittle or concrete-like materials. The inelastic deformations and microcracking are deemed to be concentrated in a narrow zone called the "process zone" or "craze", ahead of the real crack. Outside the process zone, the material is considered to be linear-elastic and isotropic whilst the locus of a potential crack is conceived to be made up of the union of crack, process zone and undamaged material.

A critical ingredient of the cohesive crack model is the description of the behavior of a generic potential crack. For a mode I crack model, as assumed herein, the following hypotheses are made. When the material is still undamaged, the normal tractions p across the potential crack locus have not yet reached some limiting tensile value p_o. In the process zone, however, a normal discontinuity of displacements w occurs when the traction attains p_o. This traction decreases with w along the process zone and becomes zero at some critical crack width w_o. An actual crack is deemed to have formed at zero traction when $w>w_o$. It is further assumed, as is commonly the case for concrete materials where aggregate interlocking is present, that the tangential displacement discontinuity is zero and that the corresponding tangential (shear) traction is unrestricted.

Within the above broad description of the cohesive crack model, two further idealizations of the constitutive behavior are possible, analogous to the deformation and flow theories of plasticity.

In the first instance, it is often assumed that the softening law is path-independent so that any stress point can only move on the softening locus $f(w)=0$. This is not strictly correct since, even under proportionally applied loads, local elastic unloading (that is a decrease in traction at constant displacement discontinuity) can still occur, as clearly illustrated by the behavior of the ubiquitous two-notch tensile test (Bolzon *et al.* 1995). In our work, we adopt the following more realistic constitutive behavior, albeit in an approximate form for computational efficiency.

The mathematically correct description of the softening law pertaining to the process zone must necessarily be expressed in rate form (time being an ordering variable). This type of history-dependent behavior is schematically illustrated in Fig. 1. It is clearly shown, through the direction of the arrows, that unloading within the process zone is correctly accounted for. For general nonlinear softening functions, it is usually difficult to solve the rate equations exactly; recourse is

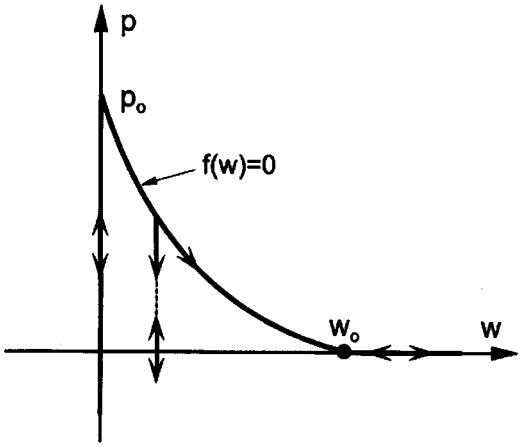

Fig. 1 Path-dependent mode I cohesive crack model

often made, as in our work, to an incremental finite step analysis consisting of a series of path-independent analyses with appropriate updating carried out at the start of each step.

Analytically, the path-dependent cohesive crack law illustrated in Fig. 1 can be written in rate form, similar to that in Bolzon *et al.* (1997), as

$$\begin{cases} \dot{w}=0,\ \dot{p}\gtrless 0, & \text{if } 0\le w\le w_o,\ y=p_o^*-p>0 \\ \dot{y}\ge 0,\ \dot{y}\,\dot{w}=0, & \text{if } 0<w\le w_o,\ y=f(w)=0 \\ \dot{w}\gtrless 0,\ \dot{p}=0, & \text{if } w_o<w \end{cases} \tag{1}$$

to describe an incremental process starting from a known situation; p_o^* is the maximum tensile stress for the particular elastic branch on which the current stress point lies, and the notation $x\gtrless 0$ is used to denote the fact that variable x is "free" or unconstrained. The first relation in (1) refers to a stress point in an "elastic" condition. That is, it describes the movement of a point either on the initial elastic branch ($w=0$, $p_o^*=p_o$) or one which has elastically unloaded from the softening curve ($0<w\le w_o$, $p_o^*<p_o$). The second condition assumes that the current stress point is "active" (i.e., is on the softening branch). The evolution of that point can follow either of two paths, as shown in Fig. 1. It can elastically unload ($\dot{w}=0$, $\dot{y}>0$) or can continue yielding down the softening curve ($\dot{w}>0$, $\dot{y}=0$). In both cases, the orthogonality condition (or "complementarity", as it is known in the mathematical programming literature) $\dot{y}\dot{w}=0$ is thus satisfied. The third condition in (1) refers to the fully cracked case and is self-evident.

Two interesting points deserve mention:

Firstly, whilst it seems reasonable, as indicated in Fig. 1, that during unloading the process zone opening w cannot decrease while the normal stress p remains tensile (assuming, in the spirit of the cohesive crack model, that the craze essentially consists of microcracks or a region of "damage", rather than an actual single crack), it is not clear whether this should also hold when p becomes compressive. Of course, if it is assumed that the process zone represents some "damage" in tension only, then unlimited compressive strength appears logical.

Secondly, the horizontal branch in Fig. 1 for $w>w_o$ shows that unloading can occur but it is unclear as to whether crack closure can be less than w_o. Our view, and one that we have

implemented in the algorithm described in a later section, is that a fully developed crack can indeed fully close. In practice, these two situations are unlikely to occur for proportionally applied loading. In fact, in all numerical examples we have run to-date, neither phenomenon has been detected.

3. Boundary element formulation

Consider the 2-dimensional body shown in Fig. 2(a) which provides a generic definition of our fracture problem. The domain Ω is subdivided into two homogeneous regions Ω^1 and Ω^2 by an *a priori* assumed locus Γ_c along which the crack will propagate. The boundary zones ($r = 1, 2$) of the structure consist of a constrained part Γ_u^r and of an unconstrained part Γ_p^r for which displacements and tractions are prescribed, respectively. Fig. 2(b) defines the local axis conventions for tangential (t) and normal (n) components of tractions and displacements for the adjacent interfaces of the two zones.

Following the elegant approach used for instance in Cen and Maier (1992), Tin-Loi and Ferris (1997) and Maier and Frangi (1998), we can describe the nonlinear response of the structure as being governed by the following integral equation:

$$p(x) = \int_{\Gamma_c} Z(x,s)w(s)d\Gamma + \mu p^e(x), \quad x, s \in \Gamma_c \tag{2}$$

where the normal tractions p on the interface Γ_c are given by the superposition of two effects: the first due to the actual normal displacement discontinuities w in the absence of any applied loads, and the second due to the external actions on an intact fully elastic structure in the absence of kinematic discontinuities. The first effect, represented by the integral term in (2), can be described through the Green's functions or influence coefficients $Z(x, s)$, $x, s \in \Gamma_c$ ($x \equiv$ field point, $s \equiv$ source point) which can be calculated from a linear elastic analysis as the normal tractions p caused by unit normal displacement discontinuities w across Γ_c in the unloaded (i.e., without any external actions) structure. The second right hand side term of (2) is simply the elastic response of the uncracked structure under the given external actions where μ is a load factor and p^e are normal elastic tractions on Γ_c for μ=1.

Conceptually, the analysis is easy. If the crack path is known, we need simply combine and

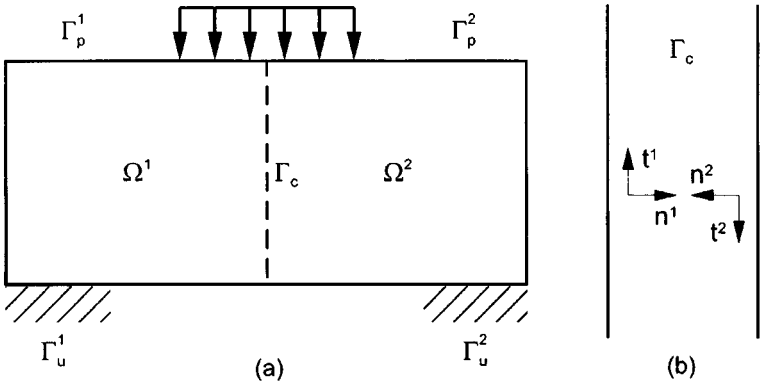

Fig. 2 Problem definition: (a) structure; (b) local axis systems at interface

solve (1) and (2) to obtain the relevant quantities of interest. Formally, however, as shown in several papers (e.g., Cen and Maier 1992, Maier and Frangi 1998), the fracture analysis is not straightforward. We are faced with two major difficulties. Firstly, even if the crack path were known in advance, solving (1) and (2) is not a simple task. Secondly, except for simple situations, the crack itinerary is unknown in advance and requires some iterative scheme to update the assumed crack interface. Before describing how we overcome both of these difficulties, we outline the calculation of the Green's functions in (2) using a standard two-zone boundary element model. Extension to more than two zones is straightforward.

Analytical expressions for $Z(x, s)$ are rarely possible so that these influence coefficients need to be calculated from a suitably space-discretized structure. Moreover, as (2) involves variables on the boundary and at the assumed interface only, a BE approach is more suitable than a FE method which would involve domain variables as well. Motivated primarily by simplicity of implementation, we adopt the direct collocation BE approach (Banerjee 1993) with isoparametric quadratic three-node boundary elements.

Starting from the well-known matrix formulation of a two-zone collocation BE method for the situation shown in Fig. 2, we can write for both domains Ω^r, $r = 1, 2$ the linear relation

$$\boldsymbol{H}^r \boldsymbol{u}^r = \boldsymbol{L}^r \boldsymbol{p}^r \tag{3}$$

where vectors $\boldsymbol{u}^r$ and $\boldsymbol{p}^r$ collect, respectively, the nodal displacements and tractions on boundaries Γ_p^r, Γ_u^r and Γ_c^r of the model; $\boldsymbol{H}^r$ and $\boldsymbol{L}^r$ are conventional nonsymmetric influence matrices obtained from appropriate integrations of the classical boundary integral equations. Bold-face symbols refer to vectors and matrices.

The boundary unknowns on Γ_p^r and Γ_u^r can now be eliminated from (3) to give the following system in variables pertaining only to the interface Γ_c:

$$\boldsymbol{p}_c^r = \boldsymbol{G}^r \boldsymbol{u}_c^r + \boldsymbol{q}^r \tag{4}$$

where quantities $\boldsymbol{G}^r$ and $\boldsymbol{q}^r$ are obvious by-products of the condensation.

Eq. (4) can be partitioned as

$$\boldsymbol{p}_c^r = [\boldsymbol{G}_n^r \;\; \boldsymbol{G}_t^r] \begin{bmatrix} \boldsymbol{u}_{cn}^r \\ \boldsymbol{u}_{ct}^r \end{bmatrix} + \boldsymbol{q}^r \tag{5}$$

before we impose to it the static-kinematic conditions which hold at the interface Γ_c, namely,

$$\boldsymbol{p}_c^1 = \boldsymbol{p}_c^2, \;\; \boldsymbol{u}_{ct}^1 = -\boldsymbol{u}_{ct}^2, \;\; \boldsymbol{u}_{cn}^1 + \boldsymbol{u}_{cn}^2 + \boldsymbol{w} = 0 \tag{6}$$

in accordance with the sign convention shown in Fig. 2(b). Simple algebraic manipulations lead to

$$\boldsymbol{p}_c^1 = -\boldsymbol{G}^1 \bar{\boldsymbol{G}}^{-1} \boldsymbol{G}_n^2 \boldsymbol{w} + \boldsymbol{G}^1 \bar{\boldsymbol{G}}^{-1} (\boldsymbol{q}^2 - \boldsymbol{q}^1) + \boldsymbol{q}^1 \tag{7}$$

where the superscript -1 denotes an inverse and

$$\bar{\boldsymbol{G}} = [(\boldsymbol{G}_n^1 + \boldsymbol{G}_n^2) \;\; (\boldsymbol{G}_t^1 + \boldsymbol{G}_t^2)] \tag{8}$$

Finally, we simply extract from Eq. (7), the normal component of p_c^1 to give an expression for the normal traction p at the interface, or

$$\boldsymbol{p} = \boldsymbol{Z}\boldsymbol{w} + \mu \boldsymbol{p}^e \tag{9}$$

which clearly is the discrete version of the integral Eq. (2). Note that we have not only obtained the influence matrix $\boldsymbol{Z}$ but also the elastic response due to the applied external actions in the absence of any displacement discontinuity.

4. Algorithm for crack propagation

In this section, we address the two major difficulties to be overcome in the crack propagation analysis, namely, solution of the path-dependent relations, Eq. (1) (appropriately collected for all nodal points) and Eq. (9) for an assumed crack locus, and the interface adjustment strategy. We focus on key ideas rather than on details of the numerical implementation.

4.1. Finite incremental solution for known crack path

This stage of the analysis is conceptually straightforward, requiring the solution of relations (1) and (9). However, the actual exact numerical solution of the rate equations is not a trivial task. In practice, we need resort to an approximate, albeit acceptable, finite step marching scheme. Within each step, path independence is assumed and any updating due to elastic local unloading is accounted for between two consecutive steps. Moreover, the solution of the appropriate finite incremental relations pertaining to the evolution for any step is still not simple. For instance, the elegant complementarity approaches (e.g., as in Bolzon *et al.* 1995, 1997, Tin-Loi and Ferris 1997, and surveyed in Maier and Frangi 1998) meet with the prime difficulty that the systems in the affine case, where the softening is linear or piecewise linear, belong to the class of problems for which no polynomial time algorithm is known to exist since a key matrix is nonsymmetric (even for a symmetric BE approach) and indefinite. This implies that it can take exponential time to determine a solution or the fact that no solution exists.

Motivated by the success of our previous work (Bolzon *et al.* 1995, 1997, Tin-Loi and Ferris 1997) in which it was observed that the starting vectors for the adopted mathematical programming (more precisely, complementarity) approach could be judiciously chosen on assumed knowledge of the crack activation sequence, we have developed a simple numerical algorithm, briefly described in the following.

In the first instance, some time discretization of the governing system (1) and (9) needs to be carried out. As in plasticity (e.g., Bird and Martin 1990, Corigliano and Perego 1993), we adopt the popular backward time integration scheme in view of its good convergence and stability properties. The entire structural evolution is then analyzed as a sequence of path-independent finite incremental problems each concerning a finite configuration change $\Delta\Sigma$ from a known state $\hat{\Sigma}$ to the required (unknown) state Σ.

A crucial element of our proposed algorithm is to consider only those relations for which the *final* unknown states belong to stress points which will become active for the applied load step $\Delta\mu$, which incidentally can be positive or negative. If we indicate this active set by $\{\alpha\}$, then we need simply solve the set of equations $y_\alpha=0$ for Δw_α. We need to emphasize that the active set $\{\alpha\}$ simply contains the indices of the nodes (node numbers) which either belong to the craze or crack with no distinction made between the two.

The difficulty of course is to have a reasonable prediction of the set $\{\alpha\}$ so that we can efficiently converge towards it. Fortunately, at variance with spreading plasticity cases, the nature

of our fracture problem is such that the active set is small for conventional load steps and is also, in view of the localized cracking, often reasonably easily predictable, at least as to its pattern and approximate elements.

To be specific in our further elaboration, let us focus on the simplest case where $f(w)$ for each node is a single linear branch with negative slope h. Then, for a generic step of our finite incremental problem, we need to calculate Δw_α so that the final stress state $y_\alpha = \hat{y}_\alpha + \Delta y_\alpha = 0$. Without going into the simple algebraic manipulations required, this consists in solving

$$y_\alpha = 0 = \begin{cases} \hat{y}_\alpha - \Delta\mu p^e_\alpha + (h_{\alpha\alpha} - Z_{\alpha\alpha})\Delta w_\alpha, & \text{if } w_i \le w_o, \quad i \in \alpha \\ \hat{y}_\alpha - \Delta\mu p^e_\alpha - Z_{\alpha\alpha}\Delta w_\alpha, & \text{if } w_i > w_o, \quad i \in \alpha \end{cases} \tag{10}$$

iteratively for a sequence of assumed $\{\alpha\}$. We use α subscripts on various quantities to denote appropriate subvectors or submatrices. For instance, $\boldsymbol{Z}_{\alpha\alpha}$ is the submatrix extracted from $\boldsymbol{Z}$ using the indices contained in the active set $\{\alpha\}$. More precisely, if, say, $\{\alpha\}=\{2, 7, 9\}$, then $\boldsymbol{Z}_{\alpha\alpha}$ is obtained by retaining the 2-nd, 7-th and 9-th rows and columns of $\boldsymbol{Z}$; similarly, $\boldsymbol{y}_\alpha$ would consist of the 2-nd, 7-th and 9-th rows of $\boldsymbol{y}$; etc.

We adopt the classical Newton's algorithm for solving the set of nonlinear Eqs. (10). The main steps of this algorithm are then as follows:

- Step 1: Guess $\{\alpha\}$ for the assumed load parameter increment $\Delta\mu$.
- Step 2: Solve (10) using Newton's method, or

$$y^k_\alpha + \nabla y^k_\alpha (\Delta w_\alpha - \Delta w^k_\alpha) = 0 \tag{11}$$

where k is an iteration number and Δy_α, the Jacobian matrix of y_α, is given by

$$\nabla y_\alpha = \begin{cases} \boldsymbol{h}_{\alpha\alpha} - \boldsymbol{Z}_{\alpha\alpha}, & \text{if } w_i \le w_o, \quad i \in \alpha \\ -\boldsymbol{Z}_{\alpha\alpha}, & \text{if } w_i > w_o, \quad i \in \alpha \end{cases} \tag{12}$$

- Step 3: If convergence then stop, else go to Step 1.

A few remarks are appropriate at this stage.

1. In our computational testing, we found this simple algorithm remarkably efficient and reasonably robust, even for the nonlinear softening case. There was no need to improve the global convergence of Newton's scheme through some line search type technique.
2. Of course, there is still the difficulty of finding the multiplicity of solutions which may exist even for a single crack. This is a far more difficult problem than determining the most likely crack activation amongst the identified ones. The latter task can be carried out using stability arguments founded on second-order work considerations, as discussed by Bazant and Cedolin (1992) and also by Maier and Frangi (1998). We must admit that, for finding multiple solutions, the currently proposed active set method is less robust than algorithms (Bolzon *et al.* 1995, 1997, Tin-Loi and Ferris 1997) based on solving the complete complementarity system. For small size problems (up to about 200 unknown crack displacements) and linear softening, the enumerative branch-and-bound scheme implemented by Bolzon *et al.* (1995) can capture all solutions which exist.
3. Updating of the set $\{\alpha\}$ after failure to converge can be judiciously carried out, as we have

done in our implementation, through knowledge of the previous iteration history. In practice, the steps can be chosen so that either no or only one additional node is activated. In fact, this will help in the crack path interface adjustment described in the following subsection. We need to stress that whilst the constitutive law (as a simple, invariably tenable, assumption when the discretization is fine enough) is satisfied pointwise (at the BE nodes), this in no way necessarily implies a constant crack extension for each load step. As indicated, it is computational advantageous to choose small enough load steps so that either no or only one node is activated. But even if only one node were activated say in a particular step, the appropriate craze size is automatically achieved as the algorithm will calculate where exactly the new activated node is on the constitutive law (i.e., the appropriate crack width at that node), and also, of course, which, if any, of the other nodes in the craze region has become fully cracked. In this manner, the change in both crack extension and craze length are captured automatically for each applied load step. Finally, it is possible through interpolation schemes, such as the one described in Bolzon *et al.* (1995, 1997), to satisfy more precisely the cohesive crack law between nodes, but in practice, with a fine enough BE (or FE) mesh, the computationally simpler pointwise constitutive enforcement scheme (Tin-Loi and Ferris 1997) is invariably as accurate.

4. Other variants of the above scheme, such as those involving a prediction of the load level $\Delta\mu$ and using some specified crack width as driving variable, are possible but our computational tests, albeit limited, have not shown any advantage. We found that use of the load increment as the driving variable did not incur great problems in spite of the fact that at some stage it requires a change in sign.
5. We finally note that updating of the active set automatically accounts for any elastic unloading at the beginning of the step.

4.2. Crack path realignment strategy

The general strategy we use is to realign the crack in a direction normal to the principal stress calculated at the *elastic* node immediately in front of the craze. In accordance with the fixed crack concept, the previous crack path is kept fixed; that is, realignment is only performed ahead of the damaged material. With reference to Fig. 3, where n nodes are assumed on the interface, the i-th node is the last one activated with the $(i+1)$-th node still intact (solid circles refer to nodes belonging to the crack-craze locus, open ones to the elastic locus). For the next realignment, the path 1 to i is kept fixed and the path $(i+1)$ to n adjusted. We keep the end node n fixed as long as possible to save on the discretization costs for the external boundary. Obviously, the assumed crack path far ahead of the current crack tip should not affect the accuracy of the scheme since that region is still in an elastic state; of crucial concern is the proper evaluation of the (elastic) stress state at the still elastic node immediately ahead of the craze tip.

At the start of the analysis, the interface is located using such information as location of notches and other defects, symmetry, structure geometry and loading, elastic stresses, etc. We assume that the crack itinerary starts from a free boundary with no traction, usually at a notch in a direction normal to the notch boundary.

For a generic realignment phase, such as from $(i+1)$ to n, we carry out a series of finite incremental steps and at the same time continuously monitor the stress state at node $(i+1)$. As soon as we detect that node $(i+1)$ is about to become active and enter the $\{\alpha\}$ set, we realign based on its (elastic) stress state.

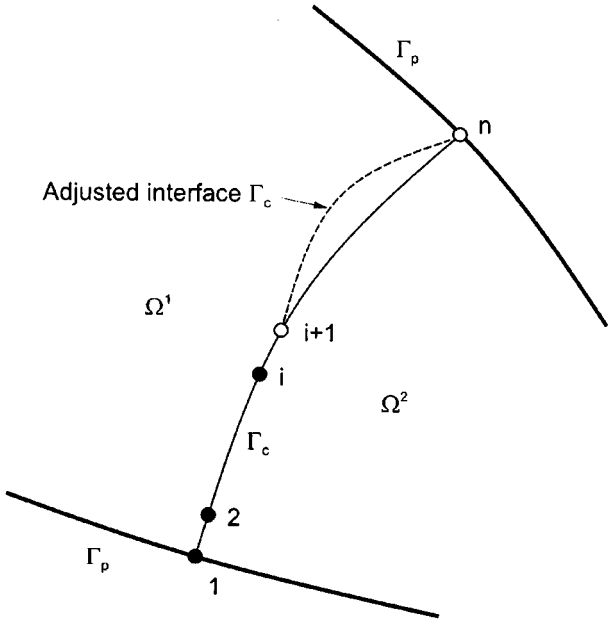

Fig. 3 Interface adjustment

An advantage of using boundary elements is that any realignment does not lead to distortion as it would for finite elements.

5. Illustrative examples

Two examples are given in this section to illustrate application of the algorithm developed. The first example is that of a tensile specimen with two semi-circular notches and for which the quasibrittle fracture law is nonlinear. The second example concerns a single edge-notched beam under four-point shear loading – an experimental set up used by Carpinteri *et al.* (1993).

5.1. Example 1

This hypothetical example involves the two-notch tensile specimen shown in Fig. 4. Overall plate dimensions are: 50 mm long, 30 mm wide and 1 mm thick. The unsymmetrically located semi-circular notches are each of 10 mm diameter. The BE model is also shown in Fig. 4 and consists of 10 matching pairs of elements on the assumed crack interface and 40 elements around the perimeter; all elements are three-noded and quadratic (midside nodes are not shown in Fig. 4).

Material data assumed are: a nonlinear cubic softening law $f(w)=p_o(1-w/w_o)^3$ with p_o=3 MPa and w_o=0.06 mm, Young's modulus E=32400 MPa and Poisson's ratio ν=0.

The load P was applied as indicated and the propagation of the crack tracked. The crack interface, as depicted, was assumed to be initially straight. The deflections u, conjugate to P, were also calculated. The final crack itinerary obtained is shown in Fig. 5. The corresponding

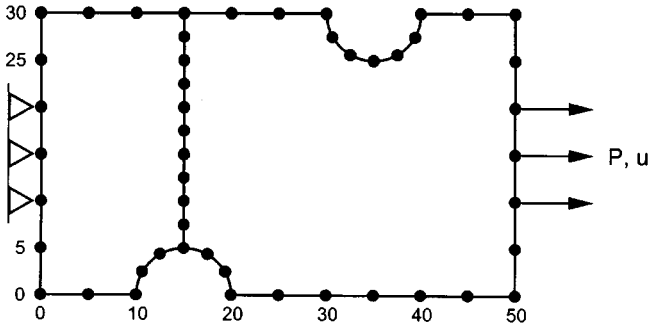

Fig. 4 Example 1: geometry and loading

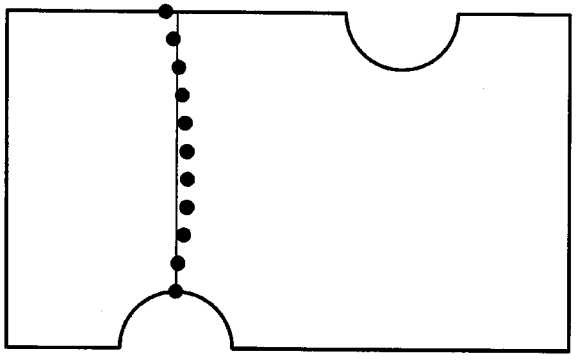

Fig. 5 Example 1: crack path evolution

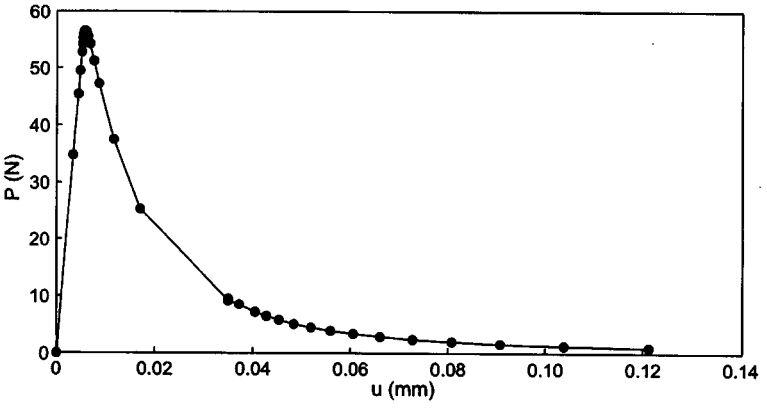

Fig. 6 Example 1: load-displacement curve

load-deflection curve is displayed in Fig. 6 which, as expected, exhibits a typical softening behavior.

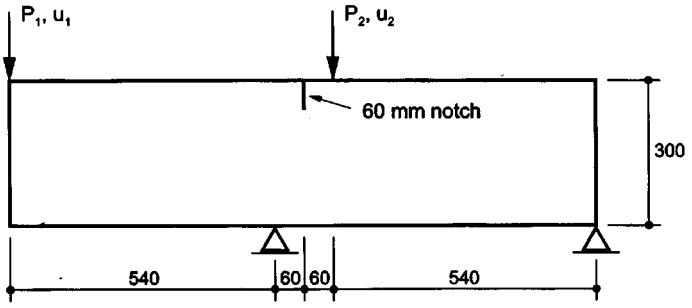

Fig. 7 Example 2: geometry and loading

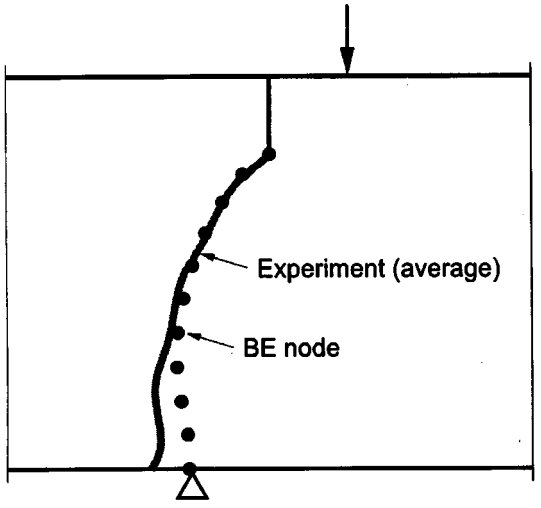

Fig. 8 Example 2: final crack path

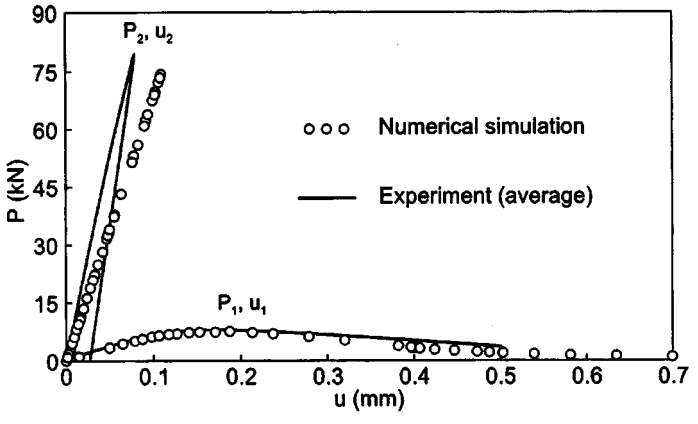

Fig. 9 Example 2: load-displacement curves

5.2. Example 2

This second example is a far better test of the procedure developed as it compares the BE solutions with results experimentally obtained by Carpinteri *et al.* (1993) for the single edge-notched specimen loaded under four point shear shown in Fig. 7. The particular details shown correspond to Specimen 2C, chosen in view of the fact that mode I fracture governs the crack propagation for that specimen.

The beam is 1200 mm long, 300 mm deep and 100 mm wide, with a 60 mm deep notch. It was loaded and supported as shown in Fig. 7 with the loads applied through a rigid beam so that P_2=10P_1. Details can be found in Carpinteri *et al.* (1993).

In our numerical simulation, we again modelled the beam with quadratic 3-noded elements, the number of which were: 40 at the top and bottom edges of the beam, 10 on the left and right vertical sides of the beam, 2 pairs of elements for the notch and 10 pairs of elements on the assumed crack interface. Except for the crack interface elements, all elements were 30 mm long.

Assumed material data are: E=40000 MPa, ν=0.1 and a single branch linear softening law $f(w)$= $p_o(1 - w/w_o)$ with p_o=2 MPa and w_o=0.125 mm. The same data were adopted by Carpinteri *et al.* (1993) in their finite element simulations of the fracture process.

The final crack interface we obtained is shown in Fig. 8 together with the average path of experimentally recorded cracks. In Fig. 9, we compare our load-deflection predictions with the average of experimentally obtained ones. In both cases, reasonable agreement can be observed. The validity of the BE analyses is further confirmed by the fact that the numerical results they provide coincide almost exactly with those given by the sophisticated, but computationally demanding, finite element approach of Carpinteri *et al.* (1993). Of particular note is the good prediction related to maximum load levels. The deviation of calculated from experimental results, as noted by Carpinteri *et al.* (1993), appear to be of the same order of magnitude as the aggregate size, except near the support. The obvious discrepancy near the support may be due to differences between the modeled simulated support conditions and the actual ones used in the experiments. It may also be possible that, in view of the complex stress state near the support, the assumed mode I law may not be fully appropriate.

6. Conclusions

A simple BE approach has been presented for carrying out the path-dependent analysis of quasibrittle fracture based on the cohesive crack model. Under the assumptions of a mode I process and unknown crack itinerary, features of the scheme involve: (a) approximation of the governing rate equations, through a backward difference scheme, as a finite incremental system; (b) solution of the system as a set of nonlinear equations characterizing the set of predicted active modes; and (c) appropriate interfacing of the marching solution with a crack alignment strategy based on the principal stresses for an intact node immediately in front of the craze.

The scheme has been found to work well on the examples ran to date, two of which are presented in this paper. The incorporation of general nonlinear softening laws does not present any difficulty and hence not only overcomes the burden of piecewise linearization but also enables extension of the method to cater for more complex mixed-mode fracture processes. The robustness of the method, however, can be improved, in particular in relation to the iterative updating of the trial active sets. This is particularly important for situations where numerous

multiple equilibrium solutions are present, as is often the case with softening induced instability. We note again that choosing the energetically critical crack among identified solutions is not difficult; the problem is to first capture the multiple solutions that may exist.

Finally, the present paper has not directly addressed the subject of interacting crack development in which multiple cracks may develop, progress simultaneously, possibly at different rates. This worthwhile extension is still possible within a multizone (with several interfaces) boundary element framework using the strategies described herein. We expect that this task will primarily involve formal rather than conceptual complications.

Acknowledgements

This research was supported by the Australian Research Council. I would also like to thank Professor G. Maier and Dr. G. Bolzon for stimulating discussions on the subject of quasibrittle fracture analysis, Professor J.S. Pang for pointing out the similarity of the complementarity algorithm with the B-diff scheme, Mr H. Li for help with numerical computations, and the reviewers for constructive comments on an earlier version of the paper.

References

Banerjee, P.K. (1993), *The Boundary Element Methods in Engineering*, McGraw-Hill, London.

Barenblatt, G.I. (1962), "The mathematical theory of equilibrium cracks in brittle fracture", *Advances in Applied Mechanics*, **7**, 55-129.

Bazant, Z.P. and Cedolin, L. (1992), *Stability of Structures: Elastic, Inelastic, Fracture, and Damage Theories*, Oxford University Press, New York.

Bird, W.W. and Martin, J.B. (1990), "Consistent predictors and the solution of the piecewise holonomic incremental problem in elasto-plasticity", *Engineering Structures*, **12**, 9-14.

Bolzon, G., Maier, G. and Tin-Loi, F. (1995), "Holonomic and nonholonomic simulations of quasi-brittle fracture: a comparative study of mathematical programming approaches", *Fracture Mechanics of Concrete Structures* (ed., F.H. Wittmann), Aedificatio Publishers, Freiburg, Germany, 885-898.

Bolzon, G., Maier, G. and Tin-Loi, F. (1997), "On multiplicity of solutions in quasi-brittle fracture computations", *Computational Mechanics*, **19**, 511-516.

Carpinteri, A., Valente, S., Ferrara, G. and Melchiorri, G. (1993), "Is mode II fracture energy a real material property?", *Computers & Structures*, **48**, 397-413.

Cen, Z. and Maier, G. (1992), "Bifurcations and instabilities in fracture of cohesive-softening structures: a boundary element analysis", *Fatigue and Fracture of Engineering Materials and Structures*, **15**, 911-928.

Corigliano, A. and Perego, U. (1993), "Generalized midpoint finite element dynamic analysis of elastoplastic systems", *International Journal of Numerical Methods in Engineering*, **36**, 361-383.

Dugdale, D.S. (1960), "Yielding of steel sheets containing slits", *Journal of the Mechanics and Physics of Solids*, **8**, 100-104.

Harder, N.A. (1990), "Computer simulated crack propagation in concrete", in *Fracture Behaviour and Design of Materials and Structures* (ed., D. Firrao), Chameleon Press, London, 706-714.

Hillerborg, A., Modeer, M. and Petersson, P.E. (1976), "Analysis of crack formation and crack growth in concrete by means of fracture mechanics and finite elements", *Cement and Concrete Research*, **6**, 773-782.

Liang, R.Y. and Li, Y.N. (1991a), "Simulations of nonlinear fracture process zone in cimentitious

material - a boundary element approach", *Computational Mechanics,* **7**, 413-427.

Liang, R.Y. and Li, Y.N. (1991b), "Study of size effect in concrete using fictitious crack model", *Journal of Engineering Mechanics, ASCE,* **117**, 1631--1651.

Maier, G. and Frangi, A. (1998), "Symmetric boundary element method for "discrete" crack modelling of fracture processes", *Computer Assisted Mechanics and Engineering Science* (forthcoming).

Tin-Loi, F. and Ferris, M.C. (1997), "Holonomic analysis of quasibrittle fracture with nonlinear softening", *Advances in Fracture Research* (eds, B.L. Karihaloo, Y.W. Mai, M.I. Ripley and R.O. Ritchie), Pergamon, Oxford, 2183-2190.